Rapid Communications | Editors' Suggestion

Low-energy electron-mode couplings in the surface bands of Sr_2RuO_4 revealed by laser-based angle-resolved photoemission spectroscopy

Shuntaro Akebi,[1] Takeshi Kondo,[1,*] Mitsuhiro Nakayama,[1] Kenta Kuroda,[1] So Kunisada,[1] Haruka Taniguchi,[2,3] Yoshiteru Maeno,[2] and Shik Shin[1]

[1]*Institute for Solid State Physics (ISSP), University of Tokyo, Kashiwa, Chiba 277-8581, Japan*

[2]*Kyoto University, Kyoto, Kyoto 606-8502, Japan*

[3]*Iwate University, Morioka, Iwate 020-0066, Japan*

(Received 26 November 2018; revised manuscript received 15 January 2019; published 7 February 2019)

We use angle-resolved photoemission spectroscopy with a 7-eV laser, which is capable of ultrahigh energy and momentum resolutions, and investigate bosonic mode couplings in the surface bands of Sr_2RuO_4. Significantly, our measurements reveal pronounced kink structures at very low binding energies (∼8 and ∼15 meV), which have a strong variation in the renormalization strength among multiple bands derived from the Ru 4*d* orbitals. Neutron scattering has observed phonon modes with the lowest energy scale around 15 meV, which thus could be the main source for the ∼15-meV kink. In contrast, the significant coupling at the lower energy (∼8 meV) is attributed to magnetic excitations, which are reported to be peaked in density of states around 10 meV. The ∼8-meV kink is found to be strongest in the two-dimensional $4d_{xy}$-derived band, implying its mechanism to be the electron coupling to ferromagnetic spin fluctuations.

DOI: 10.1103/PhysRevB.99.081108

In strongly correlated electron systems, the band structures are significantly renormalized by many-body effects due not only to electron-electron interaction, but also to the coupling of electrons with bosonic modes such as phonons and magnons [1–5]. The mode couplings are particularly interested in the study of superconductors, since these could be the essential excitations to form electron pairs in the superconducting state. An electron-boson coupling generates a bending structure (so-called "kink") in the band dispersion of materials, thus many efforts have been given to search for low energy kinks close to the Fermi energy (E_F) and identify the bosons potentially mediating the superconductivity [6].

The ruthenate oxide Sr_2RuO_4 has a perovskite layered structure with the superconducting transition at ∼1.5 K [7]. Since its discovery, this compound has gotten much attention due to the expectation of unconventional spin-triplet *p*-wave superconductivity [8,9]. Ferromagnetic (FM) spin fluctuations were originally proposed to be responsible for the formation of electron pairing [10–13]. The incommensurate peaks observed by neutron scattering, however, suggest that antiferromagnetic (AFM) correlations should not be neglected for the superconducting mechanism [14–18]. On the other hand, the angle-resolved photoemission spectroscopy (ARPES) study claims the significance of phonon couplings: the kink structure has been observed at ∼30–40, ∼50–60, and ∼70–80 meV for the bulk band [19–21], which are obviously larger than the energy scale of the reported magnetic excitations (<10 meV) [14–16], and rather agree to the energy scales for some of the optical phonons [22,23]. Therefore, it has been even suggested that the spin-triplet *p*-wave superconductivity of Sr_2RuO_4 is phonon mediated [20].

Sr_2RuO_4 has a unique crystal layer on the surface with RuO_6 octahedrons slightly rotated by ∼8° [24], differing from the bulk crystal with no such structural distortion. This is attributed to the freezing of the zone-boundary soft phonon into a static lattice distortion at the surface [22,24,25]. Calculations further predict that the consequent surface could be ferromagnetic [24], whereas the band reconstruction due to the magnetic ordering has not been observed by ARPES [26]. Nonetheless, the ferromagnetic fluctuation could be hidden and wait for high-resolution measurements to unveil its coupling to electrons. Investigation of the surface band is, moreover, important in light of the topological aspect of this compound: the edge state predicted for the topological superconductor [27–33] has been detected [34]. Intriguingly, the tunneling spectroscopy has revealed that the surface layer is superconducting [35]. Since the novel edge state should stay on the boundary between the surface and bulk, identifying the low-lying excitations related to the surface superconductivity would be crucial to understand the topological nature for the real material.

Recently, scanning tunneling spectroscopy (STS) has extracted the fine features of band structure close to E_F for the bulk and surface state from the quasiparticle interference (QPI) pattern, exhibiting the mode coupling around ∼10, ∼40, and ∼70 meV [36]. The determination of band structures with this technique is, however, limited to the one-dimensional-like (1D-like) band derived from the $d_{xz/yz}$ orbitals, since the QPI requires a good nesting of Fermi surface. To draw the full picture of mode couplings in Sr_2RuO_4, ARPES would be the most powerful probe: It allows one to directly determine all the multiple bands including the $4d_{xy}$-derived γ band, which is viewed as the active source for superconducting instability [12,13].

In this Rapid Communication, we reveal the significant electron-mode couplings in the topmost layer of Sr_2RuO_4.

*kondo1215@issp.u-tokyo.ac.jp

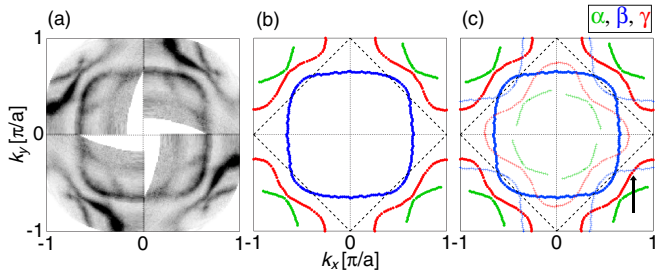

FIG. 1. (a) ARPES intensities at E_F: The strong intensities (black color) correspond to k_F points. (b) The main Fermi surface determined from the ARPES mapping in (a). (c) The main Fermi surface and that folded across the reduced zone boundary (diagonal lines) generated due to the rotation of RuO_6 octahedrons on the crystal surface. The arrow indicates the momentum cut for Fig. 2(a).

We clearly observe kink structures in band dispersions at very low binding energies (∼15 and ∼8 meV). We find that the strength of the kinks is strongly orbital dependent and anisotropic around the Fermi surface. The lowest energy of optical phonons and the cut-off energy of acoustic phonons have been estimated to be ∼15 meV by neutron-scattering experiments [22,23]. Therefore, the kink structure observed at the lower energy (∼8 meV) is attributed to the magnetic excitations, which are reported to be peaked in density of states at around 10 meV [16]. The renormalization strength across ∼8 meV is estimated to be more than twice higher in the two-dimensional $4d_{xy}$ band than in the one-dimensional $4d_{xz/yz}$-bands, suggesting that the related bosonic mode is ferromagnetic rather than antiferromagnetic.

Single crystals of Sr_2RuO_4 were grown by the floating-zone technique. ARPES measurements were performed for the (001) cleaving surface with a ScientaOmicron R4000 hemispherical analyzer with an ultraviolet 7-eV laser ($h\nu$ = 6.994 eV) at the Institute for Solid State Physics, the University of Tokyo [37]. The sample temperature and the energy resolution were set to be 5 K and 1.3 meV, respectively. The samples were cleaved *in situ* and kept under a vacuum better than 3×10^{-11} torr during the experiments.

We first demonstrate that the ARPES data measured by a 7-eV laser ARPES selectively observe the electronic structure for the topmost layer of Sr_2RuO_4 crystal, which is reconstructed by the RuO_6 rotation [38]. Figure 1(a) plots the ARPES intensities at the Fermi energy (E_F); the strong intensities (black color) correspond to the k_F points. In Fig. 1(b), the Fermi surfaces (FSs) of the main bands are determined from the peak positions of spectra. The α and β FSs derived from the $d_{xz/yz}$ orbitals, and the γ FS from the d_{xy} orbital are plotted with green, blue, and red filled circles, respectively. Differently from the γ FS for the bulk state with an electronlike shape centered at (0,0), our data exhibit a holelike γ FS centered at the zone corner (π, π), which is a hallmark for the surface state [26,39,40]. This variation of FS topology from bulk to surface is caused by a relative energy shift of the saddle point at (π,0) from above to below E_F due to the crystal distortion [38,41]. The RuO_6 rotation of crystal on the surface enlarges the unit cell by $\sqrt{2} \times \sqrt{2}$, which reduces the size of the Brillouin zone (dashed black lines in Fig. 1) [24,25]. We confirm that the complex FSs mixed by the main

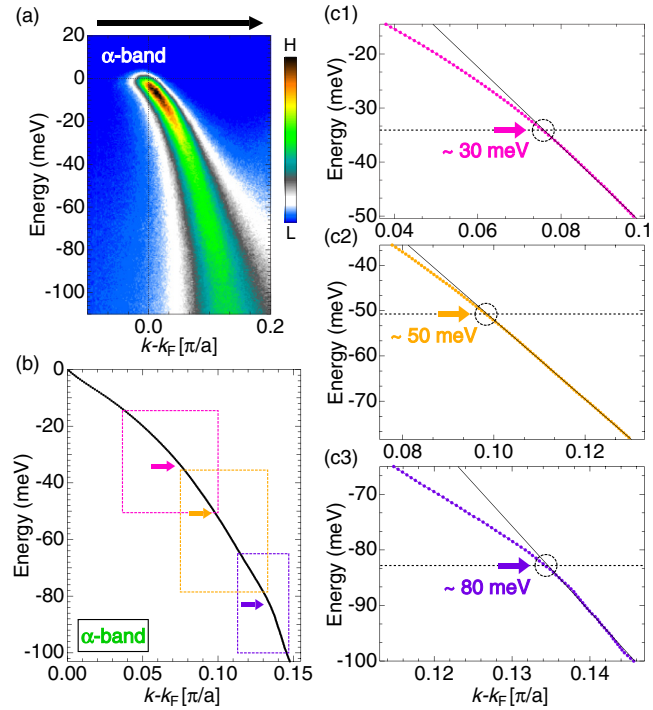

FIG. 2. (a) ARPES dispersion for the α band measured along the momentum cut indicated by an arrow in Fig. 1(c). (b) Band dispersion determined from the peak positions of MDCs extracted from the image in (a). Magnified dispersion of (b), demonstrating kink structures at ∼30 meV (c1), ∼50 meV (c2), and ∼80 meV (c3), which are pointed to by arrows. The energy windows for these panels are marked in (b) with dashed rectangles. Each solid black line is fit to the data at binding energies higher than the kink energy.

FSs and those reflected across the reduced zones [Fig. 1(c)] well reproduce the ARPES data [Fig. 1(a)].

In passing, we emphasize that our data exhibit only the signature of the topmost RuO_6 layer, and free from that of the second layer, which causes additional band splitting [40,42]: While the γ FS in the second layer of crystal was found to have an electronlike shape similar to that of the underlying bulk system, we observe only the holelike γ FS, indicating that the 7-eV laser ARPES is selective of the topmost-layer state due to a matrix element effect [38].

Here we show that all the mode couplings reported so far for Sr_2RuO_4 through ARPES study are observed in our data measured by laser ARPES. Now we focus on the α band, which is free from the complex overlapping of multiple bands due to the band folding, thus easily determined up to high binding energies. Figure 2(a) presents the ARPES dispersion measured along the momentum cut indicated by an arrow in Fig. 1(b). In Fig. 2(b), we determine the band dispersion from the peak positions of momentum distribution curves (MDCs) extracted from the ARPES image of Fig. 2(a) for each different binding energy up to 100 meV. We find kink structures at several energies along the band dispersion, signifying the strong coupling of quasiparticles with multiple collective modes. To estimate the kink energies, we zoom the dispersion in Figs. 2(c1)–2(c3) within three different energy windows [red, green, and blue dashed squares indicated in

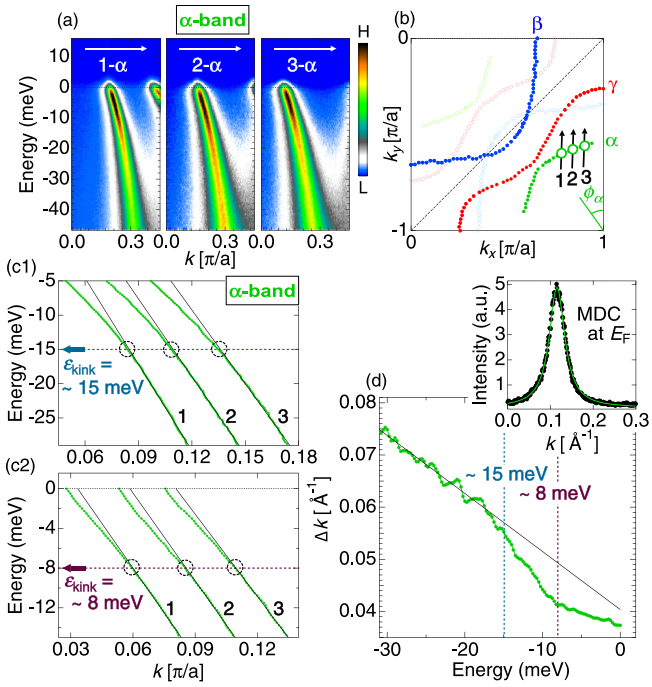

FIG. 3. (a) ARPES dispersions (1-α, 2-α, and 3-α) for the α band obtained along three-momentum cuts indicated by arrows in (b). (b) Fermi surface determined by ARPES with measured momentum cuts for (a). (c1) The band dispersions determined from MDC peaks over a narrow energy window around the kink energy of ~15 meV. (c2) The similar data to (c1), but plotted around the kink energy of ~8 meV. The solid black lines in (c1) and (c2) are fit to the data at binding energies higher than the kink energies. (d) The momentum width of MDCs (Δk) for different energies. In the inset, a typical MDC at E_F is extracted from the image of (a). The data is fit to the Lorenz function (a green curve).

Fig. 2(b), respectively]; we have identified significant variations in group velocity across ~30, ~50, and ~80 meV. The electron-phonon couplings at these three energies have been reported before for the bulk state measured by the synchrotron ARPES [19,20], indicating that the phonon excitations are common for the surface and the bulk.

The laser ARPES has excellent energy and momentum resolutions, thus it has the capability of unveiling kink structures closer to the Fermi level [37]. In Fig. 3, we demonstrate that the α-band dispersions [Fig. 3(a)] exhibit significant kinks at two low binding energies of ~15 [Fig. 3(c1)] and ~8 meV [Fig. 3(c2)]. The spectra of the α band are not contaminated from the intensities of the other bands, thus the MDCs extracted from the ARPES image have a clean symmetric shape [the inset of Fig. 3(d)], which can be fit well to the Lorentzian function (a green curve). This situation enables one to extract not only the peak positions but also the intrinsic spectral widths (Δks), which are plotted in Fig. 3(d) for different binding energies. We find the remarkable sharpening of spectra (or decreasing of Δk) below ~15 meV, which corresponds to the kink energy ($\varepsilon_{\rm kink}$) [see Fig. 3(c1)]. The same effect for the other coupling at $\varepsilon_{\rm kink} = \sim 8$ meV is not clearly visible in the $\Delta k(\varepsilon)$ plots, while a kinklike anomaly is seen at this energy. Note that the peak positions of MDCs [$\varepsilon(k)$'s] are more accurate to reveal anomalies in the band dispersion, thus we have used these, rather than $\Delta k(\varepsilon)$'s, to identify the energies of mode couplings, following the previous ARPES reports [3,20].

We have also examined the band renormalization effect in the other bands (the γ and β bands) in the vicinity of E_F. In order to properly determine the band dispersions, we focus on the momentum space [black lines in Fig. 4(b)] where the spectral intensities for folded bands are rather weak, thus have little influence on the analysis of MDC fitting. The ARPES images obtained are exhibited in Figs. 4(a1)–4(a11), in which the dispersions for β and γ bands are both captured. In Figs. 4(c1) and 4(c2) and Figs. 4(d1) and 4(d2), we determine the β and γ dispersions, respectively, which are marked by arrows (1-β to 6-β and 6-γ to 11-γ) in Figs. 4(a1)–4(a11). Significantly, the kink structures are identified again at two low energies (~15 and ~8 meV), which are the same as those for the α band. To confirm that the kink behavior especially of the γ band is not just an artifact coming from the inherent band shape, we superimpose the density functional theory (DFT) band in Figs. 4(a6)–4(a9), which can be viewed as the bare band with no many-body effect; it shows a linear dispersion without any indication of bending, strongly contrasting to the ARPES data.

Whereas the kink structures at the two energy scales (~15 and ~8 meV) are commonly observed for all the multiple bands, the renormalization strength (λ) is found to be strongly orbital dependent and anisotropic around each Fermi surface. In Figs. 4(e1) and 4(e2), we estimate the value of λ from the velocity change ($v_1/v_0 = \lambda + 1$) across the coupling energy: here v_0 and v_1 are the slopes of band dispersion above and below the kink energy, respectively. The obtained values for all three bands are compared in Figs. 4(e1) and 4(e2). We find that the renormalization effect is more pronounced at ~15 than at ~8 meV for all the directions observed. Interestingly, the magnitude of λ for the ~15-meV kink is comparable between the β and γ bands, likely because the FSs for these two bands are adjacent in momentum space, giving rise to mutual interactions. This circumstance causes similarly anisotropic λ's in these bands, in contrast to the isotropic λ's in the α band, which is well isolated in the momentum space.

A promising mechanism on the ~15-meV kink is the electron-phonon coupling [22,23,43]. Note that the kink structure is expected to appear around the energies of optical phonons and/or the cut-off energy of acoustic phonons strongly coupled to the electrons of matter [44]. Importantly, the phonon dispersion of Sr_2RuO_4 determined by neutron scattering signifies that the lowest magnitude of such energies is ~15 meV; these phonon modes have been observed along almost every direction, in agreement with our ARPES results [22,23]. In addition, this situation indicates that the kink structure in bands at lower binding energies than ~15 meV require different kinds of excitations other than phonons.

The band renormalization at ~8 meV becomes weakest in the β band among the three bands [Fig. 4(e2)], contrasting to that at ~15 meV with the largest λ in the same band [Fig. 4(e1)]. This clear distinction in the orbital dependence implies that the mode couplings at these two energies have different origins. Neutron-scattering experiments suggest that the bosons with energies lower than ~10 meV in Sr_2RuO_4

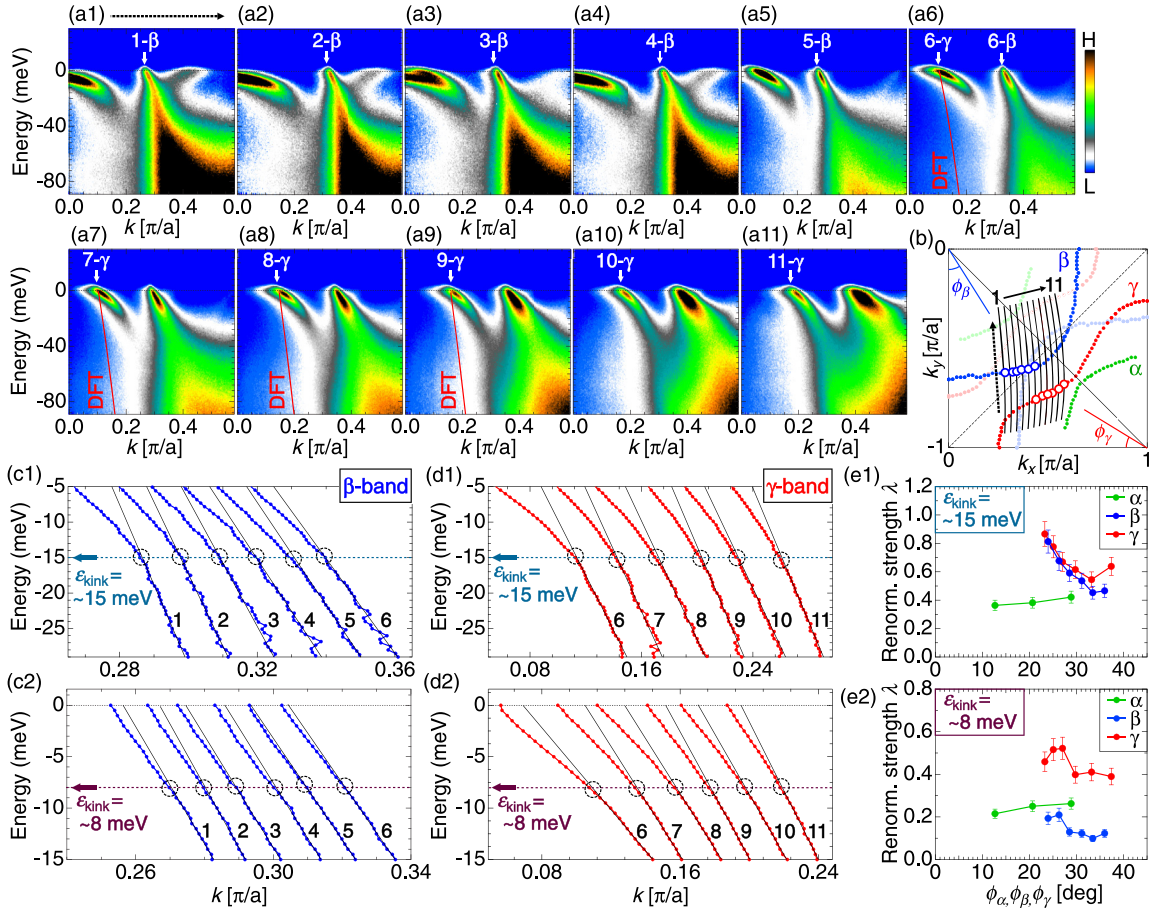

FIG. 4. (a1)–(a11) ARPES dispersions for the β and γ bands obtained along the momentum cuts indicated in (b). The red lines in (a6)–(a9) indicate the DFT dispersions for the γ band [38]. (b) Fermi surface determined by ARPES with measured momentum cuts. (c1),(c2) The dispersions of the β band determined by MDC peaks over a narrow energy window around the kink energy of ∼15 and ∼8 meV, respectively. The corresponding bands and k_F points are marked by white arrows (1-β to 6-β) in (a1)–(a6) and white circles in (b), respectively. (d1),(d2) The same data as (c1) and (c2), but for the γ band [marked as 6-γ to 11-γ in (a6)–(a11)]. The solid black lines in (c1),(c2) and (d1),(d2) are fit to the data at binding energies higher than the kink energies. (e1),(e2) The strength of band renormalization, λ, estimated from the velocity change ($v_1/v_0 = \lambda + 1$) across the kink energy of ∼15 and ∼8 meV, respectively.

could be magnetic excitations; while the Σ_3 phonon mode seems to also have such low energies, the structural rotation of the RuO_6 octahedron is attributed to the softening of this mode, thus the strong coupling of surface state to it is less likely [22–24].

Incommensurate antiferromagnetic fluctuation is detected at low energies (< 10 meV), which agrees to the lowest energy (∼8 meV) of kink structure we observed [14–16]. While this excitation expects a good nesting of Fermi surface, and it is favorable for the α and β FS with 1D-like character, our data exhibit even stronger kink structure in the γ band with a two-dimensional character, which is thus incompatible with this scenario.

The FM fluctuation could be an alternative, dominant mechanism for the mode coupling at ∼8 meV. First-principle calculations suggest that a bulk soft-phonon mode freezes into a static lattice distortion associated with an in-plane rotation of the RuO_6 octahedron, and it establishes a ferromagnetic ground state on the surface [24]. The ARPES data of the surface state, however, does not show an indication of the long-range FM ordering [26]. Instead, the relevant excitations (or FM fluctuation) could be enhanced, and coupled to the quasiparticles, generating the significant kink structure as we observed: the γ band, which is mostly responsible for FM fluctuation due to high density of states near E_F, is effectively narrowed by the RuO_6 rotation [41], further increasing the FM instability through the Stoner-type mechanism as demonstrated by local-density approximation calculations [45].

In conclusion, we used 7-eV laser ARPES with ultrahigh energy and momentum resolutions, and investigated electron-boson couplings close to the Fermi energy in the topmost layer of Sr_2RuO_4. We have not only detected all the mode couplings reported before through the ARPES studies, but also revealed kink structures at much lower binding energies, which are strongly orbital dependent and anisotropic around the Femi surface. The coupling at ∼8 meV is found to be strongest in the $4d_{xy}$-derived γ band, implying its mechanism to be the ferromagnetic excitations. Since the crystal distortion on the crystal surface (i.e., the RuO_6 rotation) can increase the FM instability, the mode coupling we observed might be more pronounced than that realized in the bulk band, thus we cannot simply conclude that FM fluctuation is essential for the

superconductivity in this compound. However, our results leave the FM fluctuation as a promising candidate for the pairing mechanism against the previous assertion of phonon-mediated superconductivity by ARPES studies, which captured kink structures only at higher energy scales corresponding to the phonon modes.

We thank K. Okazaki for useful discussions. This work was supported by the JSPS KAKENHI (Grants No. JP16H00979, No. JP15H05852, No. JP17J09173, No. JP16K13829, No. JP16H02209, No. JP18H01165, and No. JP17K14319), and the JSPS-EPSRC Core-to-Core program.

[1] A. Kaminski, M. Randeria, J. C. Campuzano, M. R. Norman, H. Fretwell, J. Mesot, T. Sato, T. Takahashi, and K. Kadowaki, Phys. Rev. Lett. **86**, 1070 (2001).
[2] A. Lanzara, P. Bogdanov, X. Zhou, S. Kellar, D. Feng, E. Lu, T. Yoshida, H. Eisaki, A. Fujimori, K. Kishio, J. I. Shimoyama, T. Nodak, S. Uchidak, Z. Hussain, and Z. X. Shen, Nature (London) **412**, 510 (2001).
[3] Y. Aiura, Y. Yoshida, I. Hase, S. I. Ikeda, M. Higashiguchi, X. Y. Cui, K. Shimada, H. Namatame, M. Taniguchi, and H. Bando, Phys. Rev. Lett. **93**, 117005 (2004).
[4] K. Byczuk, M. Kollar, K. Held, Y.-F. Yang, I. Nekrasov, T. Pruschke, and D. Vollhardt, Nat. Phys. **3**, 168 (2007).
[5] M. Kim, J. Mravlje, M. Ferrero, O. Parcollet, and A. Georges, Phys. Rev. Lett. **120**, 126401 (2018).
[6] J. P. Carbotte, T. Timusk, and J. Hwang, Rep. Prog. Phys. **74**, 066501 (2011).
[7] Y. Maeno, H. Hashimoto, K. Yoshida, S. Nishizaki, T. Fujita, J. G. Bednorz, and F. Lichtenberg, Nature (London) **372**, 532 (1994).
[8] K. Ishida, H. Mukuda, Y. Kitaoka, K. Asayama, Z. Q. Mao, and Y. M. Y. Maeno, Nature (London) **396**, 658 (1998).
[9] Y. Maeno, Phys. Today **54** (1), 42 (2001).
[10] T. Imai, A. W. Hunt, K. R. Thurber, and F. C. Chou, Phys. Rev. Lett. **81**, 3006 (1998).
[11] A. P. Mackenzie and Y. Maeno, Rev. Mod. Phys. **75**, 657 (2003).
[12] M. E. Zhitomirsky and T. M. Rice, Phys. Rev. Lett. **87**, 057001 (2001).
[13] I. I. Mazin and D. J. Singh, Phys. Rev. Lett. **79**, 733 (1997).
[14] M. Braden, Y. Sidis, P. Bourges, P. Pfeuty, J. Kulda, Z. Mao, and Y. Maeno, Phys. Rev. B **66**, 064522 (2002).
[15] K. Iida, M. Kofu, N. Katayama, J. Lee, R. Kajimoto, Y. Inamura, M. Nakamura, M. Arai, Y. Yoshida, M. Fujita, K. Yamada, and S. H. Lee, Phys. Rev. B **84**, 060402 (2011).
[16] P. Steffens, Y. Sidis, J. Kulda, Z. Mao, Y. Maeno, I. I. Mazin, and M. Braden, arXiv:1808.05855.
[17] I. I. Mazin and D. J. Singh, Phys. Rev. Lett. **82**, 4324 (1999).
[18] D. Manske, I. Eremin, and K. H. Bennemann, Phys. Rev. B **67**, 134520 (2003).
[19] H. Iwasawa, Y. Aiura, T. Saitoh, I. Hase, S. I. Ikeda, Y. Yoshida, H. Bando, M. Higashiguchi, Y. Miura, X. Y. Cui, K. Shimada, H. Namatame, and M. Taniguchi, Phys. Rev. B **72**, 104514 (2005).
[20] H. Iwasawa, Y. Yoshida, I. Hase, S. Koikegami, H. Hayashi, J. Jiang, K. Shimada, H. Namatame, M. Taniguchi, and Y. Aiura, Phys. Rev. Lett. **105**, 226406 (2010).
[21] N. J. C. Ingle, K. M. Shen, F. Baumberger, W. Meevasana, D. H. Lu, Z. X. Shen, S. Nakatsuji, Z. Q. Mao, Y. Maeno, T. Kimura, and Y. Tokura, Phys. Rev. B **72**, 205114 (2005).
[22] M. Braden, W. Reichardt, S. Nishizaki, Y. Mori, and Y. Maeno, Phys. Rev. B **57**, 1236 (1998).
[23] M. Braden, W. Reichardt, Y. Sidis, Z. Mao, and Y. Maeno, Phys. Rev. B **76**, 014505 (2007).
[24] R. Matzdorf, Z. Fang, J. Zhang, T. Kimura, Y. Tokura, K. Terakura, and E. W. Plummer, Science **289**, 746 (2000).
[25] R. G. Moore, V. B. Nascimento, J. Zhang, J. Rundgren, R. Jin, D. Mandrus, and E. W. Plummer, Phys. Rev. Lett. **100**, 066102 (2008).
[26] K. M. Shen, A. Damascelli, D. H. Lu, N. P. Armitage, F. Ronning, D. L. Feng, C. Kim, Z. X. Shen, D. J. Singh, I. I. Mazin, S. Nakatsuji, Z. Q. Mao, Y. Maeno, T. Kimura, and Y. Tokura, Phys. Rev. B **64**, 180502 (2001).
[27] Y. Ueno, A. Yamakage, Y. Tanaka, and M. Sato, Phys. Rev. Lett. **111**, 087002 (2013).
[28] Y. Tanaka, T. Yokoyama, and N. Nagaosa, Phys. Rev. Lett. **103**, 107002 (2009).
[29] A. R. Akhmerov, J. Nilsson, and C. W. J. Beenakker, Phys. Rev. Lett. **102**, 216404 (2009).
[30] Y. E. Kraus, A. Auerbach, H. A. Fertig, and S. H. Simon, Phys. Rev. Lett. **101**, 267002 (2008).
[31] L. Fu and C. L. Kane, Phys. Rev. Lett. **100**, 096407 (2008).
[32] C. J. Bolech and E. Demler, Phys. Rev. Lett. **98**, 237002 (2007).
[33] C. W. J. Beenakker, Annu. Rev. Condens. Matter Phys. **4**, 113 (2013).
[34] S. Kashiwaya, H. Kashiwaya, H. Kambara, T. Furuta, H. Yaguchi, Y. Tanaka, and Y. Maeno, Phys. Rev. Lett. **107**, 077003 (2011).
[35] I. A. Firmo, S. Lederer, C. Lupien, A. P. Mackenzie, J. C. Davis, and S. A. Kivelson, Phys. Rev. B **88**, 134521 (2013).
[36] Z. Wang, D. Walkup, P. Derry, T. Scaffidi, M. Rak, S. Vig, A. Kogar, I. Zeljkovic, A. Husain, L. H. Santos, Y. Wang, A. Damascelli, Y. Maeno, P. Abbamonte, E. Fradkin, and V. Madhavan, Nat. Phys. **13**, 799 (2017).
[37] T. Kiss, T. Shimojima, K. Ishizaka, A. Chainani, T. Togashi, X.-Y. Wang, C.-T. Chen, S. Watanabe, and S. Shin, Rev. Sci. Instrum. **79**, 023106 (2008).
[38] T. Kondo, M. Ochi, M. Nakayama, H. Taniguchi, S. Akebi, K. Kuroda, M. Arita, S. Sakai, H. Namatame, M. Taniguchi, Y. Maeno, R. Arita, and S. Shin, Phys. Rev. Lett. **117**, 247001 (2016).
[39] A. Damascelli, D. H. Lu, K. M. Shen, N. P. Armitage, F. Ronning, D. L. Feng, C. Kim, Z. X. Shen, T. Kimura, Y. Tokura, Z. Q. Mao, and Y. Maeno, Phys. Rev. Lett. **85**, 5194 (2000).
[40] C. N. Veenstra, Z. H. Zhu, B. Ludbrook, M. Capsoni, G. Levy, A. Nicolaou, J. A. Rosen, R. Comin, S. Kittaka, Y. Maeno,

I. S. Elfimov, and A. Damascelli, Phys. Rev. Lett. **110**, 097004 (2013).

[41] E. Ko, B. J. Kim, C. Kim, and H. J. Choi, Phys. Rev. Lett. **98**, 226401 (2007).

[42] V. B. Zabolotnyy, E. Carleschi, T. K. Kim, A. A. Kordyuk, J. Trinckauf, J. Geck, D. Evtushinsky, B. P. Doyle, R. Fittipaldi, M. Cuoco, A. Vecchione, B. Büchner, and S. V. Borisenko, New J. Phys. **14**, 063039 (2012).

[43] V. B. Zabolotnyy, D. V. Evtushinsky, A. A. Kordyuk, T. K. Kim, E. Carleschi, B. P. Doyle, R. Fittipaldi, M. Cuoco, A. Vecchione, and S. V. Borisenko, J. Electron Spectrosc. Relat. Phenom. **191**, 48 (2013).

[44] S. Verga, A. Knigavko, and F. Marsiglio, Phys. Rev. B **67**, 054503 (2003).

[45] Z. Fang and K. Terakura, Phys. Rev. B **64**, 020509 (2001).